P 4(4) THE HYDROMET DECISION SUPPORT SYSTEM: TECHNOLOGY TRANSFER FROM RESEACH TO INTERNATIONAL OPERATIONS

J. William Conway, Beth Clarke, Chris Porter, Michael D. Eilts

Weather Decision Technologies, Inc.
201 David L. Boren Blvd, Suite 270, Norman, Oklahoma, USA
Phone: 405-579-7675, Fax: 405-579-7800, Contact: bconway@wdtinc.com

ABSTRACT

Weather Decision Technologies Inc. (WDT) is a private company that specializes in meteorological data integration, algorithms, and technology transer with regard to the latest state-of-the-science developments in the fields of meteorology and hydrometeorology. WDT has developed and deployed a HydroMet Decision Support System (HDSS) in several locations both in the U.S. and internationally. HDSS integrates weather radars, satellite, rain gauges, NWP, and other data sources to provide high resolution and high quality Nowcasting, Quantitative Precipitation Estimation (QPE), and Quantitative Precipitation Forecasts (QPF) in real-time. Several key technologies utilized within HDSS are licensed from leading R&D organiztions such as the U.S. National Severe Storms Laboratory and the McGill University of Canada. The HDSS contains several components such as data quality control, radar mosaics, gauge corrected QPE, flash flood prediction, automated alerting of hazardous conditions, and customized displays. Data and products from HDSS can be served to customized Web-based applications and mobile devices. This paper describes the process of data integration within HDSS, associated algorithms, and displays using our international installations as examples.

1) INTRODUCTION

Weather Decision Technologies (WDT) has licensed and integrated the latest state-of-the-science technologies from agencies such as the US National Severe Storms Laboratory (NSSL), McGill University of Canada, MIT Lincoln Laboratories, and the University of Oklahoma into a turnkey system termed the HydroMet Decision Support System (HDSS). HDSS integrates a number of data sources, processes these data through Nowcasting and

hydrometeorlogical algorithms, and serves data and products to customized displays. Results of HDSS ingest and processing can also be served to customized Web-based applications and mobile devices for various clients and consumers.

The components of the HDSS include:

- radar data quality control including clutter removal and the use of terrain and hybrid scans
- 3D mosaicking of all available radars
- production of Quantitative Precipitation Estimations (QPE) from the mosaic data
- analysis of rain gauge data and the use of those data in correction of radar derived QPE
- production of forecasts of radar reflectivity fields using the McGill Algorithm for Nowcasting Precipitation Using Semi-Lagrangian Extrapolation (MAPLE)
- derivation of QPF fields using the results of MAPLE
- a Flash Flood Prediction Algorithm (FFPA) which combines QPE and QPF values to forecast flash flood areas based on basin Flash Flood Guidance (FFG) values
- cell and attribute tracking using the Storm Cell Identification and Tracking (SCIT) algorithm
- lightning location and prediction using lightning density grids and output from MAPLE
- automated alerting of weather hazards for customer assets using the GIS-based Asset Monitoring System (GAMS)
- customized Web based display systems

Data and product outputs are available via customized web pages and a three-dimensional graphical workstation. Figure 1 shows the general HDSS concept with integration of all available data sources, the processing of those data in algorithms, and the serving of the data and products via customized interfaces.

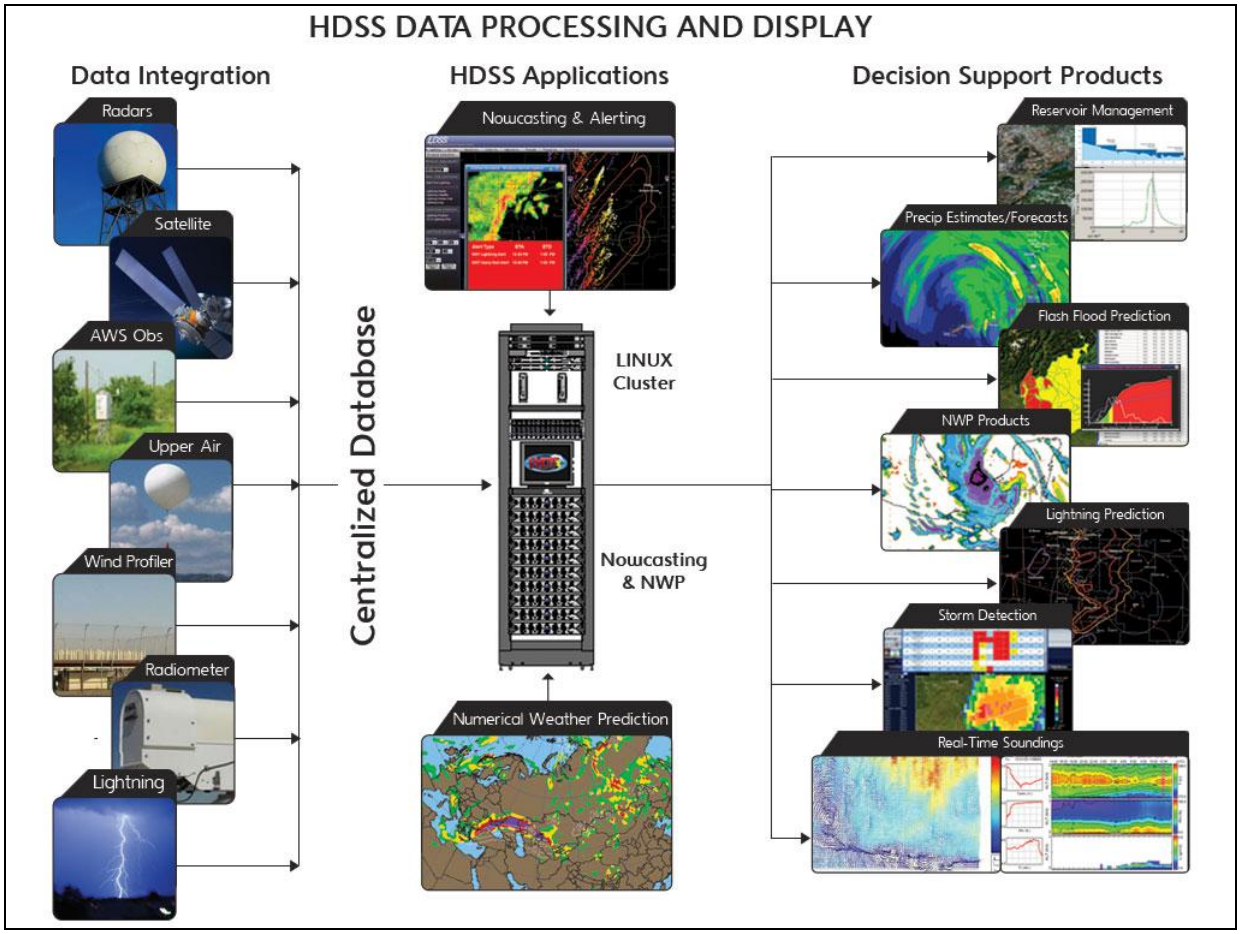

Figure 1. HDSS data integration and Nowcast flow diagram.

2) HDSS COMPONENTS

2.1 Radar Data Quality Control Algorithm (RDQCA)

The RDQCA was developed by the NSSL as part of the WDSS-II package. This algorithm ingests high resolution raw radar dual-polarization fields and performs quality control on each individual radar. This is very important in order to produce clean radar mosaics. Non-weather radar returns/echoes contaminate radar data and can be misinterpreted as real echoes by algorithms, leading to significant problems in algorithm results. The RDQCA uses several steps to perform quality control on the individual radars including the use of a neural network.

Steps contained in the RDQCA are:

a. Terrain blockages are removed - only beam clearance >50 m (adaptable parameter) and beam blockage <50% allowed to contain radar reflectivity echoes.

b. Speckle filter - range gates are pre-classified so that echo size less than a threshold value will be removed.
c. Noise removal is performed - reflectivity below noise thresholds are removed
d. Sun strobes and test patterns are eliminated - each radial is checked for reflectivity fill >90% and correlation coefficient >0.80.
e. Non-precipitation echoes are removed - echo top thresholds are applied to consider only radar echo where the height of echo top is greater than a threshold height as precipitation.
f. Attenuation correction depending on the radar wavelength.

Once these steps are performed the data are passed to a neural network. Several horizontal and vertical features of the radar data are used to discriminate between precipitating and non-precipitating radar echo. The neural network has been trained to recognize non-precipitation echo using a number of radar data characteristics such as vertical gradient and square-to-square gate differences by training on numerous cases of “bad” radar data, which included biological targets, electronic interference patterns, anomalous propagation, ground clutter and chaff. Figure 2 shows examples of the RDQCA processing applied to a US WSR-88D S-band radar. Figures 2a and 2b and 2c and 2d show before and after images of the raw data and the data after application of the RDQCA. Figure 3 shows this same algorithm applied to an EEC C-band radar in Jakarta as part of a WDT project.

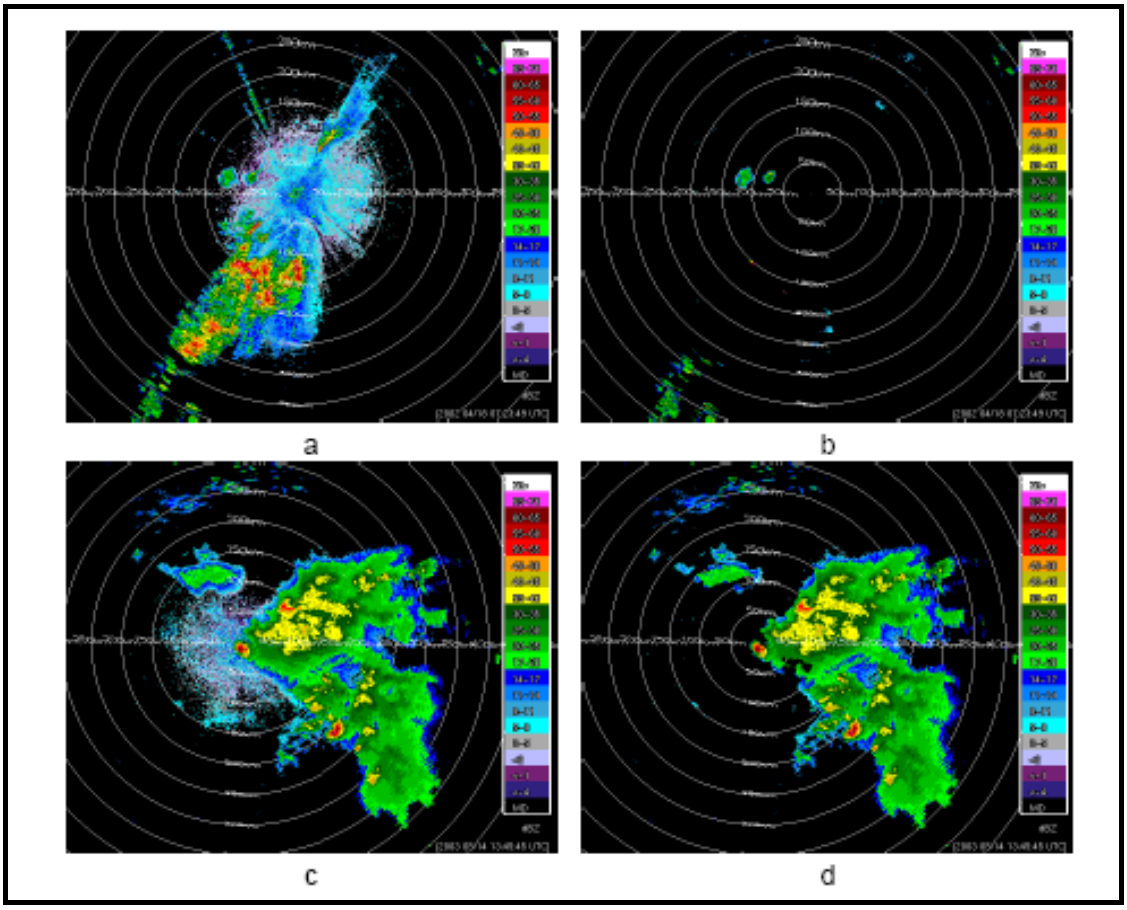

Figure 2. Examples of RDQC processing. Images (a) and (b) and images (c) and (d) show before and after results of the RDQC respectively on data from a WSR-88D radar.

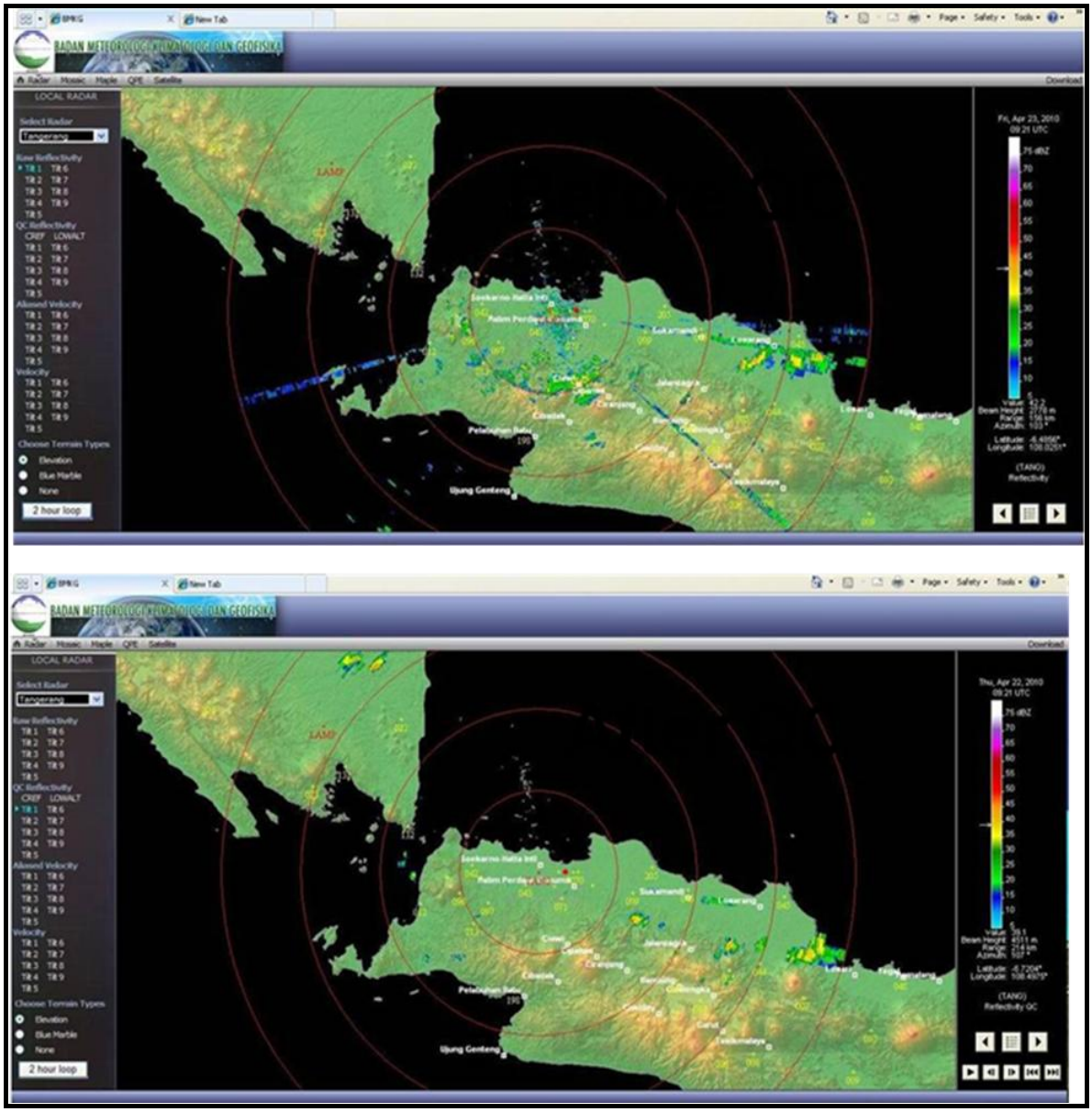

Figure 3. Examples of RDQC processing on data from an EEC C-band radar in Jakarta. Top/bottom images show data before/after RDQC application.

2.2 Three-Dimensional Radar Mosaic Algorithm

After the RDQCA algorithm is applied to each single radar volume of data, the radar data are translated to a high-resolution three-dimensional grid. Numerous products can be derived from this grid including composite reflectivity, Echo Tops Heights and Lowest Altitude reflectivity. The grid has a spacing of 500 m or 1 km and is updated as new radar volumes become available. This mosaic algorithm being proposed has been developed by the NSSL as part of WDSS-II.

The steps of the mosaic processing are:

a. Virtual volumes are first created. Each range gate from the radar with a valid value instigates the creation of an intelligent agent. When an agent is created it extracts information from the radial including its coordinates in the radar-centric spherical coordinate system (range, azimuth and elevation angle), the radial start time and the radar the observation came from. The agent transforms this information to data on coordinates in the earth-centric latitude/longitude/height coordinate system assuming a standard atmosphere. The data from each radar are re-sampled from their native polar coordinates to a regular Cartesian grid. Whenever a new elevation scan is received from any radars contributing to the 3D grid, a set of agents are created. The elevation scan radials are filtered to fit the 1km resolution of the target 3D grid using a moving average. A nearest neighbor approach is applied in the azimuth and range direction. In the elevation direction a weighting function is used to determine the value of reflectivity between two elevation scans. All interpolation methods are computed in the spherical coordinate system to remove artifacts that arise due the nature of the radar beam geometry.

b. Spatial interpolation is performed through objective analysis techniques to combine data from the multiple radars onto one grid. The radar data are weighted using an exponential weighting function. This allows radars closer to a grid point to have more influence on that point. The weighted sum of all observations that impact a cell is computed for the 3D grid. The combination of data from multiple radars using a weighted average computed in real-time establishes an automated redundancy should radar outages occur and also mitigates calibration differences between adjacent radars.

Figure 4 shows an example of this mosaic processing using the WSR-88D radars that cover the continental U.S. Figures 5 and 6 show examples of US mosaics, both with and without application of the RDQCA algorithm. Note in both figures the large amount of ground clutter, anomalous propagation, and the presence of test patterns and sun spikes that have been eliminated through the use of the RDQC algorithm. Figure 7 shows an example of the mosaic processing applied to a radar integration project in Indonesia.

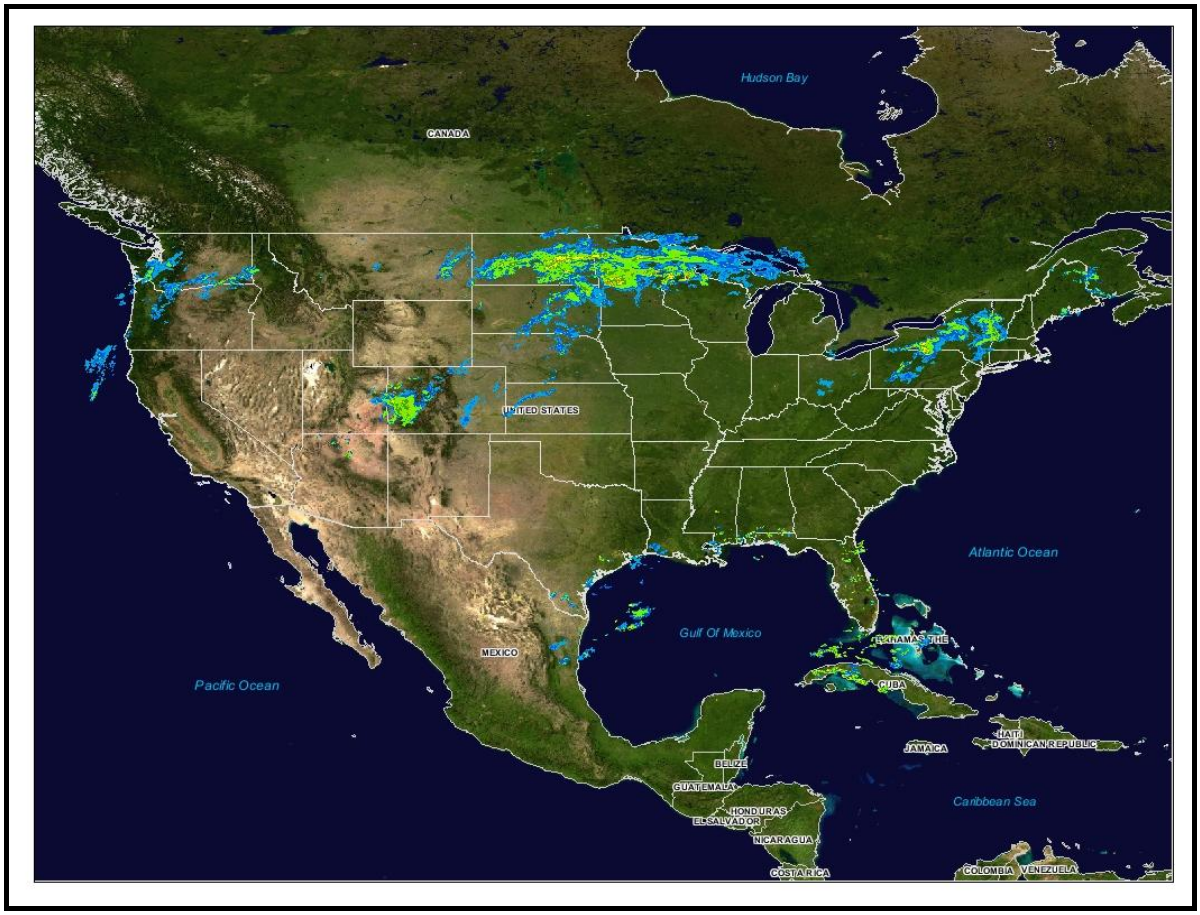

Figure 4. Example of WDSS-II mosaic processing using all WSR-88D radars that cover the continental U.S.

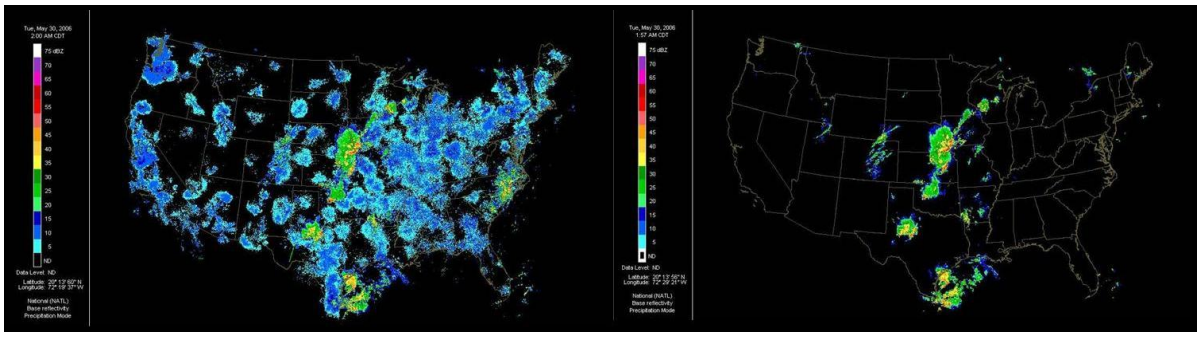

Figure 5. Example of mosaic without application of RDQCA (left panel) and mosaic after application of RDQCA (right panel).

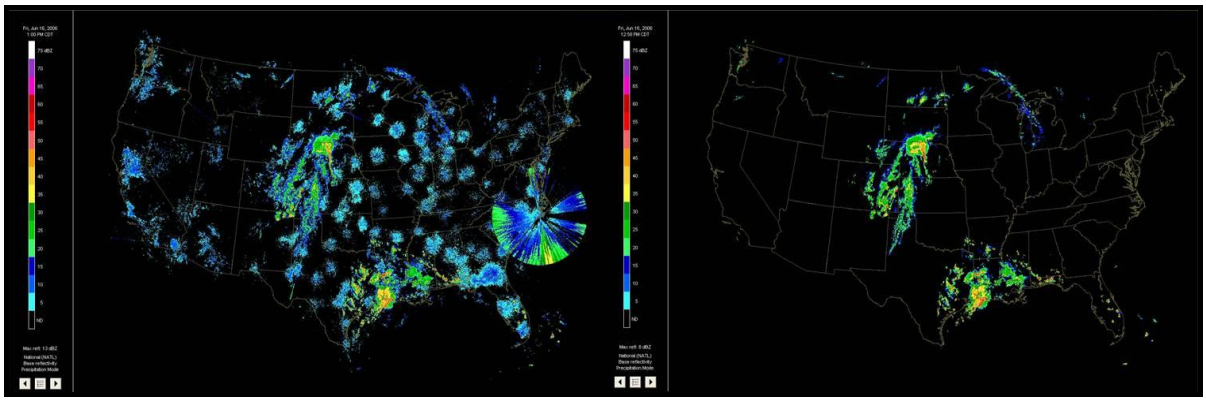

Figure 6. Example of mosaic without application of RDQCA (left panel) and mosaic after application of RDQCA (right panel).

Figure 7. Example of quality controlled mosaic produced over Indonesia.

2.3 McGill Algorithm for Precipitation Nowcasting Using Semi-Lagrangian Extrapolation

WDT has licensed from McGill University a patented software system that predicts the evolution and movement of mosaic reflectivity fields out to four hours in advance depending on the size of the domain. The algorithm, called the McGill Algorithm for Precipitatioin Nowcasting Using Semi-Lagrangian Extrapolation (MAPLE), is a sophisticated expert system/artificial intelligence application that was designed, developed and thoroughly tuned and tested by a group of scientists at McGill University over a 10-year period. WDT holds the exclusive worldwide rights for implementation of MAPLE.

An example of a vector field derived from MAPLE is shown in Figure 8. In this figure the vectors have been derived using only past mosaic reflectivity fields. Derived vector fields such as that in Figure 8 are then applied to the current mosaic reflectivity fields to produce

forecasts of reflectivity location and configuration. Figure 9 shows an example of MAPLE reflectivity forecasts with the actual reflectivity field valid for the given forecast time. Note that the location and shape of the forecasted reflectivity fields closely resemble the actual reflectivity fields valid for the same time.

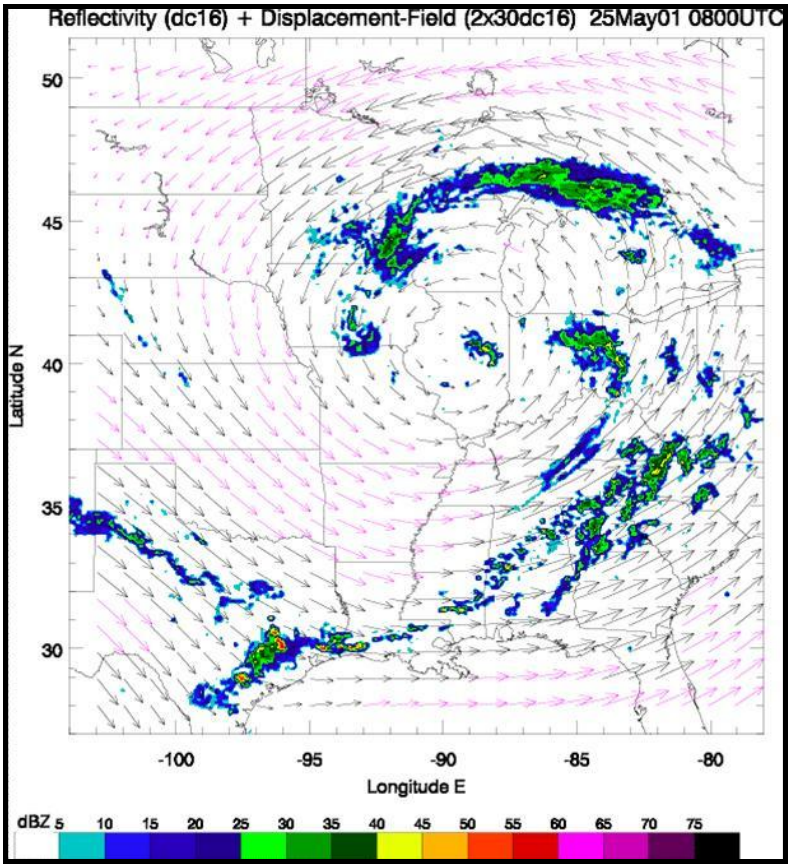

Figure 8. Example of vectors derived by MAPLE using past radar mosaics over the US.

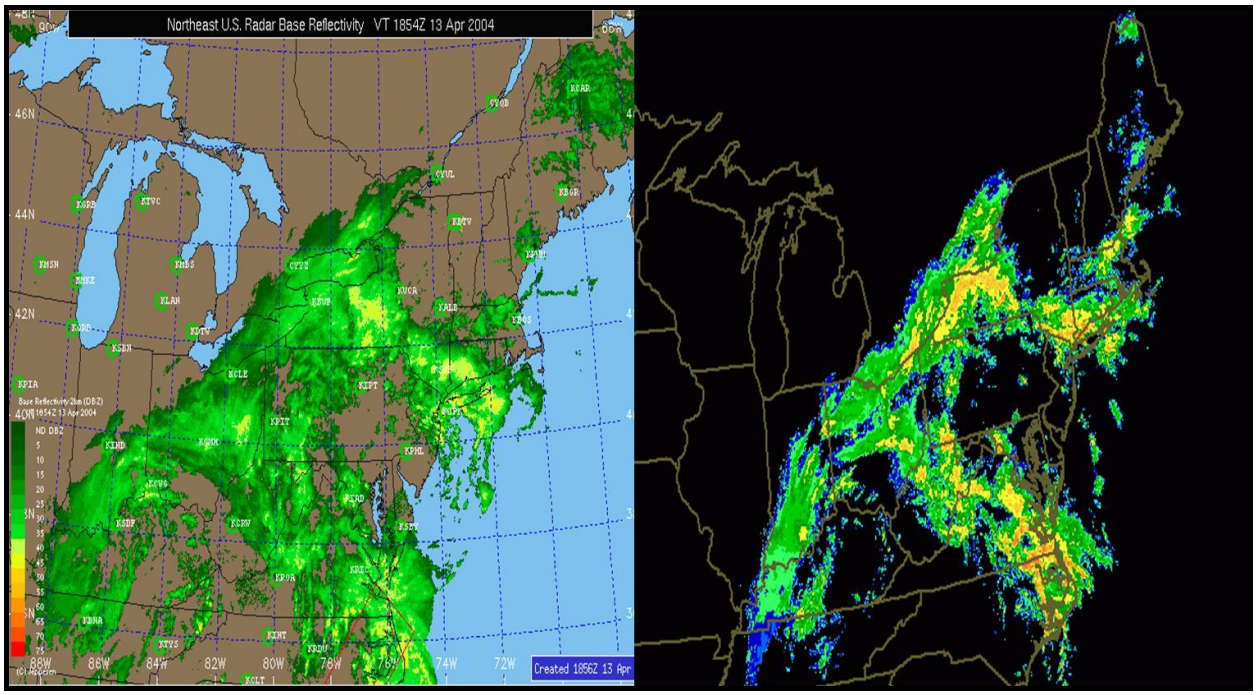

Figure 9. Example of MAPLE output over the northeastern US. The left panel shows a 2 hour MAPLE forecast while the right panel shows the actual data for this forecast.

The capability to predict rainfall accumulations (QPF) based on MAPLE forecasts is an important component of the HDSS. These rainfall forecasts are generated by utilizing a four hour-long sequence of five-minute forecasted radar images from MAPLE, converting all radar echoes to rainfall using a variable reflectivity to rain rate (Z/R) relationship, and summing the five-minute images to derive accumulated rainfall in the coming one to four hour period. Figure 10 shows an example of a 4 hour rainfall accumulation forecast from MAPLE over the US and Figure 11 shows a 4 hour accumulation forecast over Indonesia.

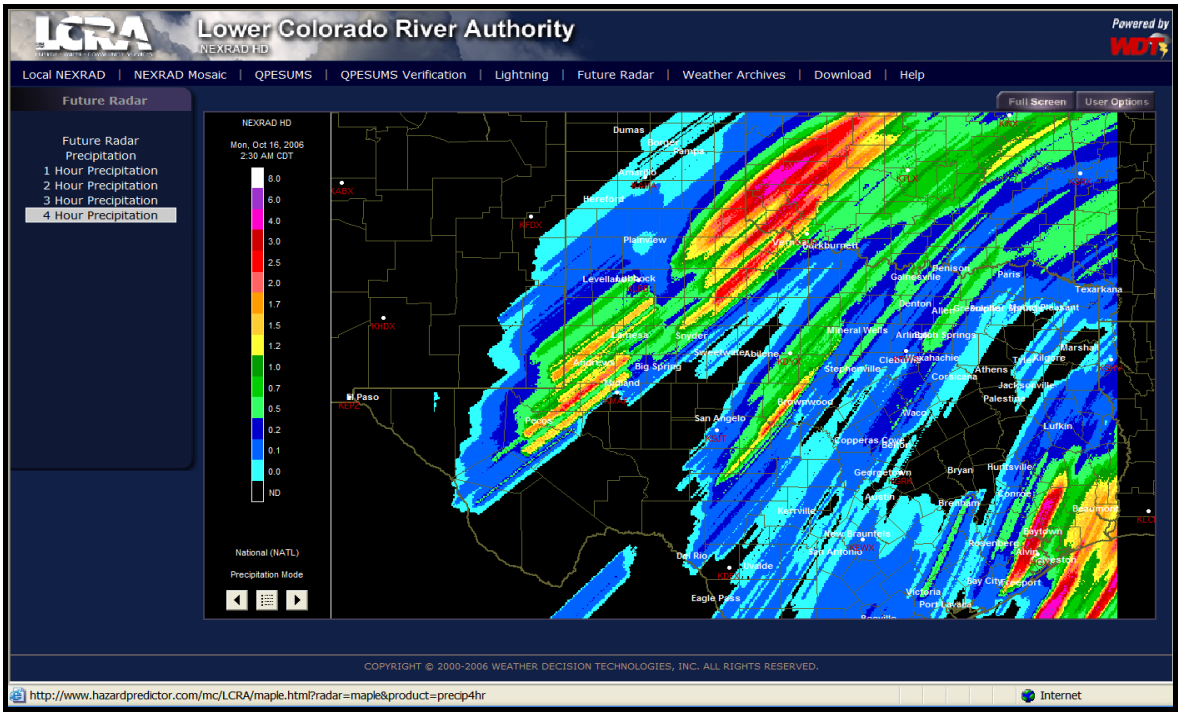

Figure 10. Example of rainfall forecast over LCRA in southern Texas. The image shows the total rainfall accumulation forecasted over a 4 hour period.

Figure 21. Example of 4 hour rainfall forecast over Indonesia.

2.4 The Quantitative Precipitation Estimation Algorithm (QPEA)

The Quantitative Precipitation Estimation Algorithm (QPEA) is a radar processing package that estimates total rainfall for the previous 72 hour period by integrating radar and rain gauge data. Results of QPEA are also provided to the Flash Flood Forecasting Algorithm as

discussed below. The following steps are performed to estimate as closely as possible the amount of rainfall at the surface:

a. QPEA uses the 3D volume of radar data to determine areas of convective and stratiform precipitation by determining if each echo has vertical extent or not.
b. Calculates QPE from the 3-D Mosaic output using several dual-polarization based pre-defined Z-R relationships.
c. Performs an objective analysis on the available rain gauge data.
d. Compares the radar derived estimates to the rain gauge analysis to determine biases in the radar data.
a. Can use a combination of satellite (if available in a timely manner) and gauge data to fill in areas where radar data are not available.
b. Corrects the radar derived rainfall estimates based on the gauge measurements.

Figure 12 shows an example of QPE over a one hour period over northern Italy.

Figure 12. Example of rain estimates for a one hour time frame from QPEA. Green lines show the basin delineation over the region.

Figure 13 shows an example a rain gauge objective analysis over the Lower Colorado River Authority area of responsibility in southern Texas. The upper left panel shows the rain gauge locations and the delineated basins. The lower right panel shows the objective analysis of the gauge data. This objective analysis is compared to the radar derived QPE and biases are computed between the two. The biases are then applied to the radar derived QPE.

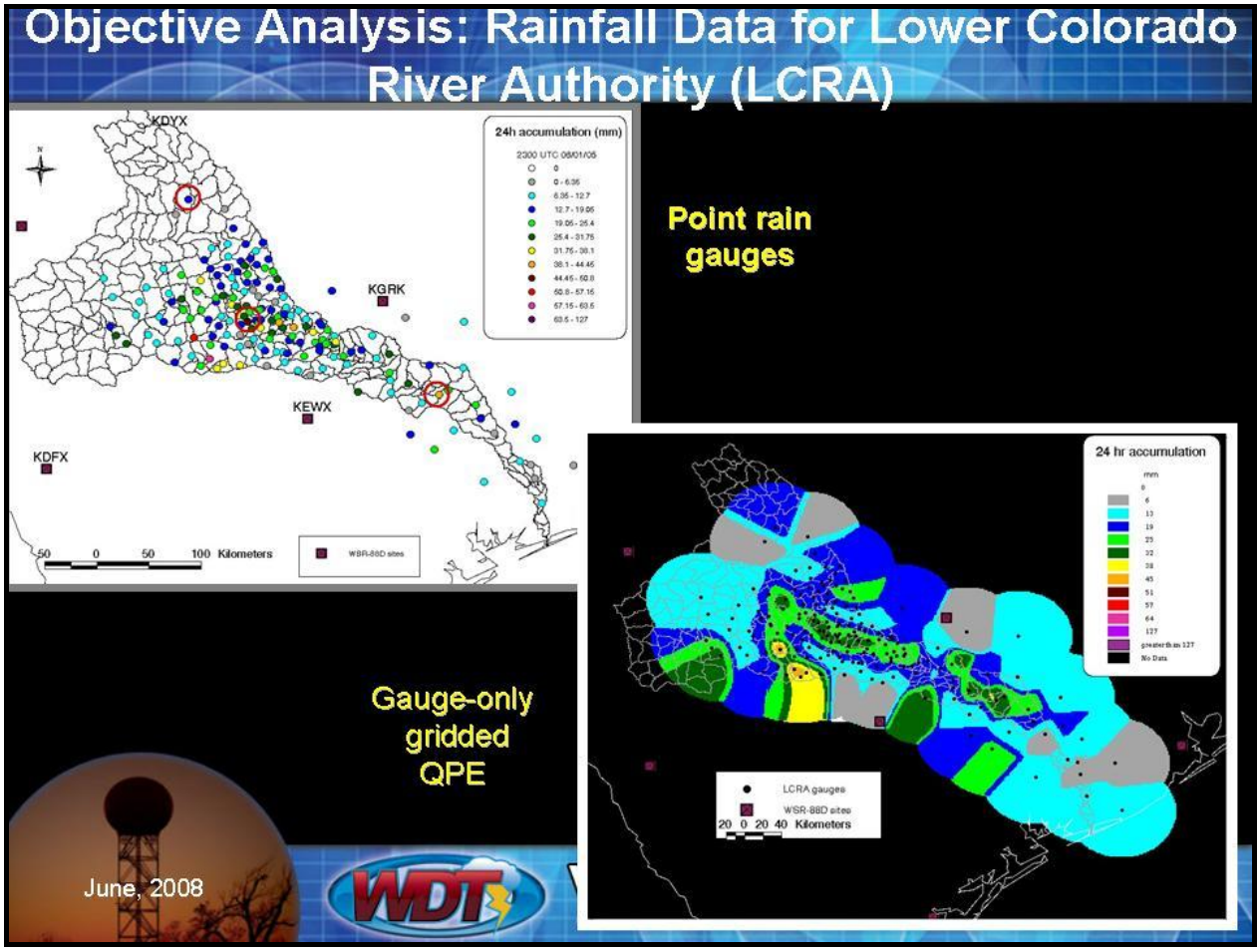

Figure 13. Implementation at LCRA in the US. Upper left panel shows delineated basins and rain gauge locations over region of responsibility. Lower right panel shows results of objective analysis of rain gauges.

Figure 14 shows an example of the radar derived QPE field averaged over pre-defined basins over the Lower Colorado River Authority region in southern Texas. This field has been corrected for rain gauge biases and has been quantified on a total basin average QPE. Results from the basin average QPE and the results from basin averaged QPF derived from MAPLE are combined to continually monitor the total past and future rainfall accumulation in each delineated basin and to warn of possible flash floods.

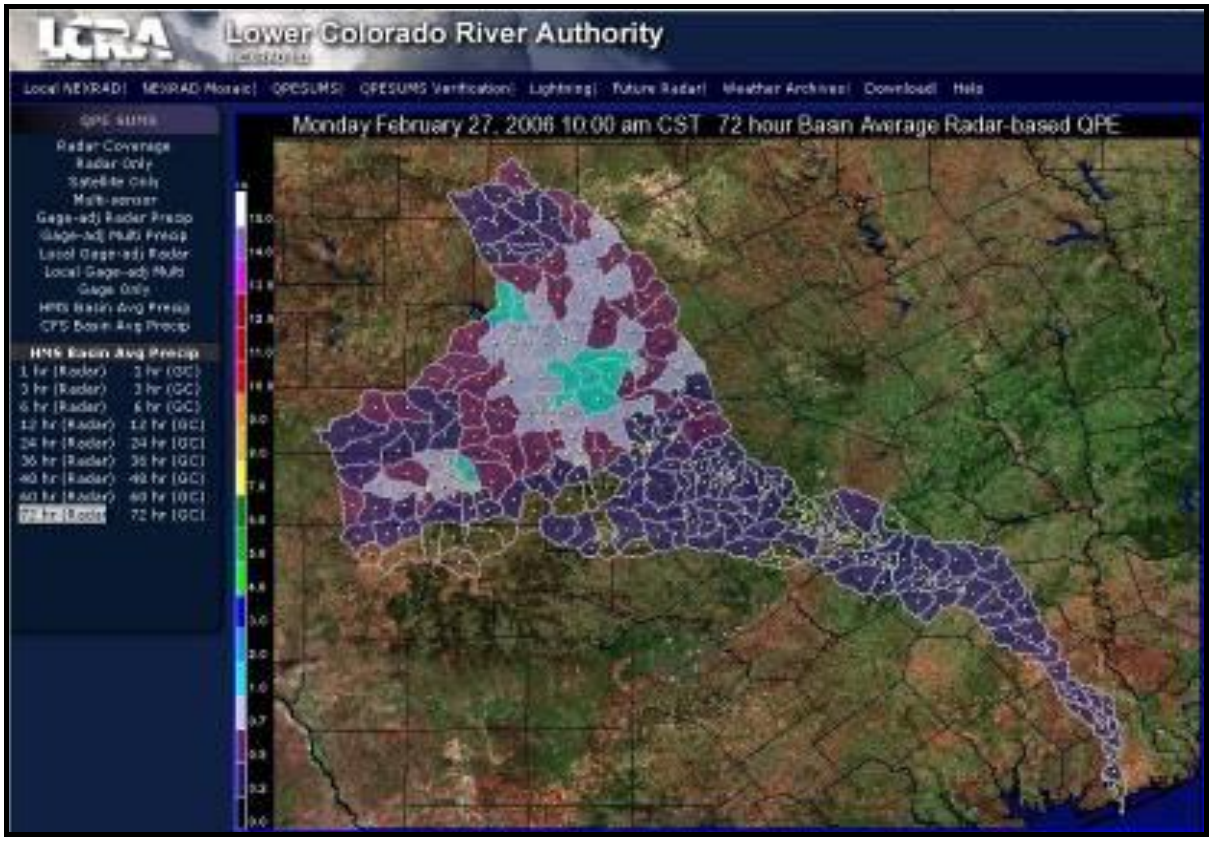

Figure 14. Radar basin average precipitation estimates that have been corrected for rain gauge biases.

2.5 Flash Flood Prediction Algorithm (FFPA)

HDSS contains a proprietary Flash Flood Prediction Algorithm (FFPA) that utilizes delineated basins covering a region as a basis for flash flood monitoring. FFPA combines output from MAPLE and QPEA to provide as accurate as possible total forecast rainfall accumulation for each basin. The FFPA compares the forecast basin accumulation against Flash Flood Guidance (FFG) values for each basin. Warnings are automatically generated for basins whose total accumulations are approaching or exceeding FFG values of if they are forecasted to exceed FFG values. Figure 15 shows an example of FFPA output. The figure shows a table of color coded basins, a basin map, and a hydrograph of one of the basins. The table and basin map show the basins that are approaching (yellow) or exceeding (red) FFG values. The user can choose a basin from the map and display a hydrograph for that basin.

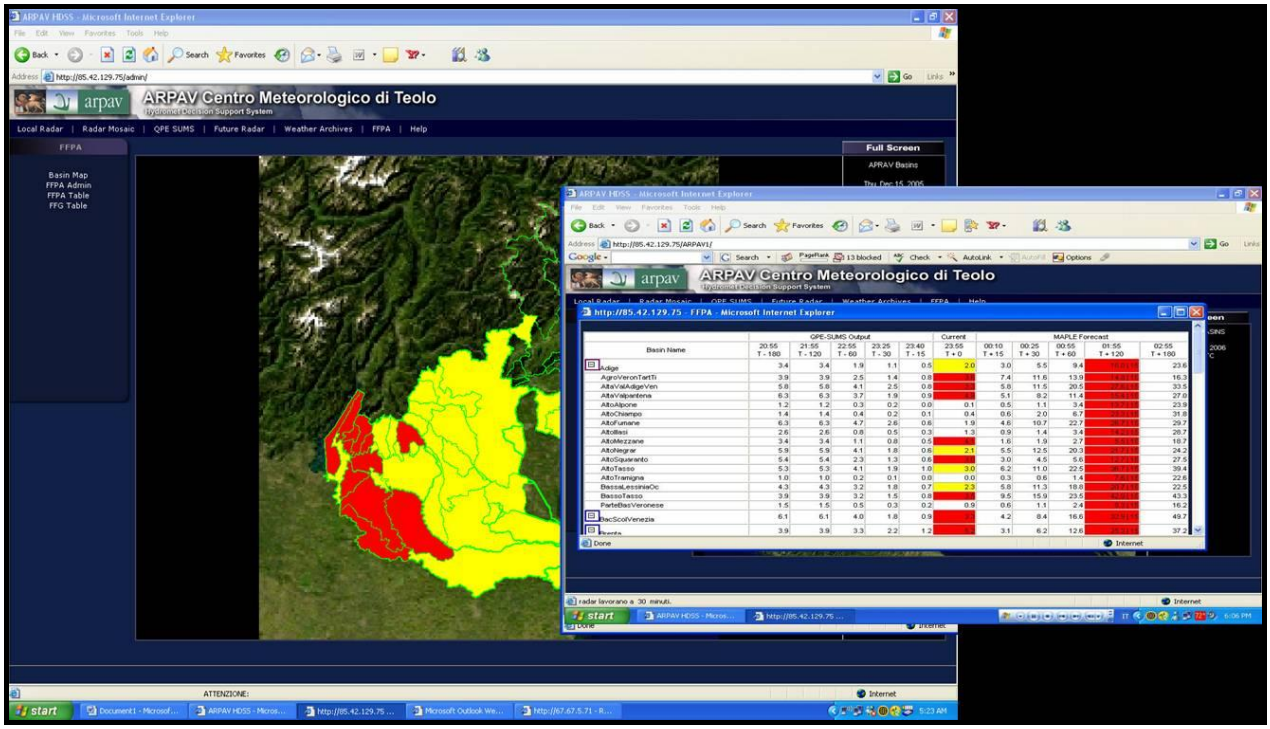

Figure 15. Example of FFPA graphical output. The table shows information on individual basins. The map shows the basin delineations. Color coding represents basins that are approaching (yellow) or exceeding (red) FFG values.

Figure 16 shows an example of the QPE/QPF table from the FFPA. The data from the table come from the FFPA database. Stored in this database are the past 72 hours of rainfall accumulation from QPEA in each delineated basin, the 3 hour accumulations that are forecast by MAPLE, and the user provided FFG values for each basin. The user has the ability through the interface shown in Figure 17 to change the FFG thresholds for each basin according to their perception and experience of what the thresholds should be for each basin over each given time period.

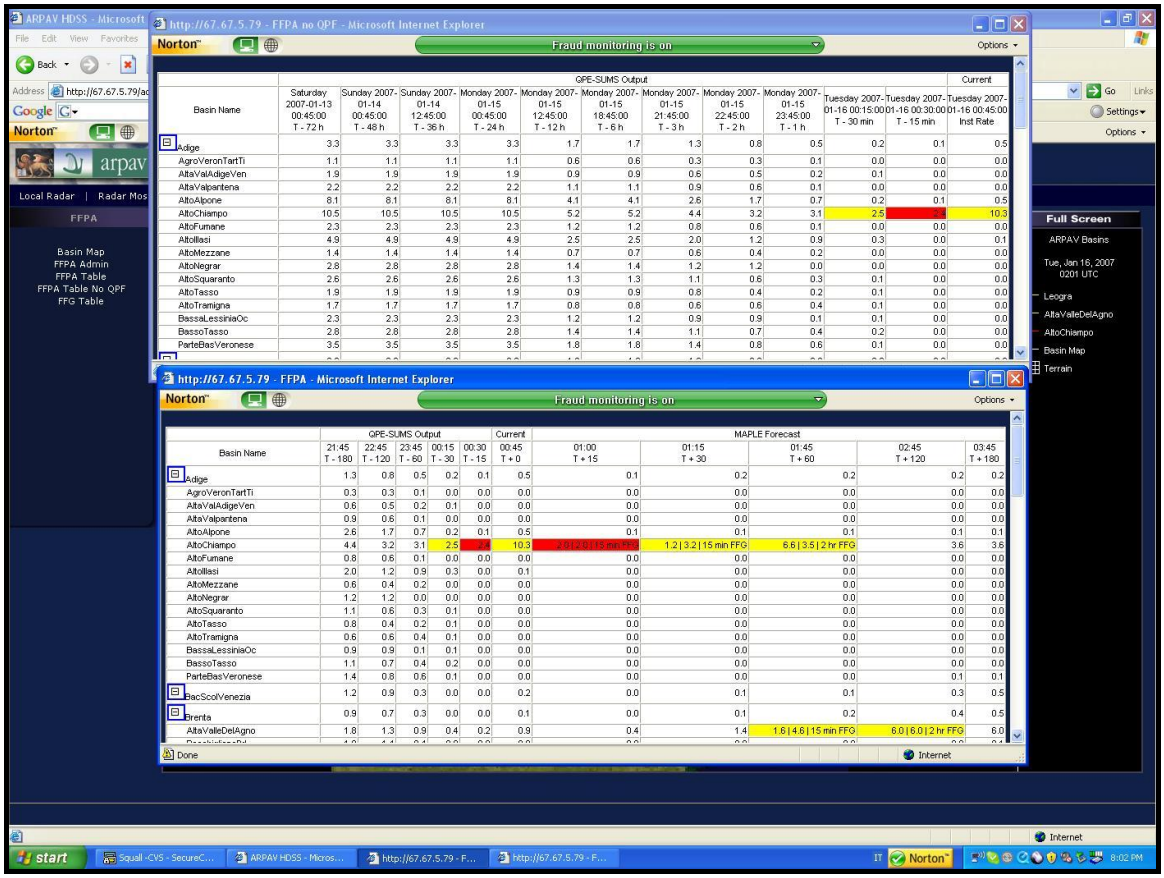

Figure 16. FFPA table showing QPEA output combined with MAPLE QPF output for several basins over northern Italy.

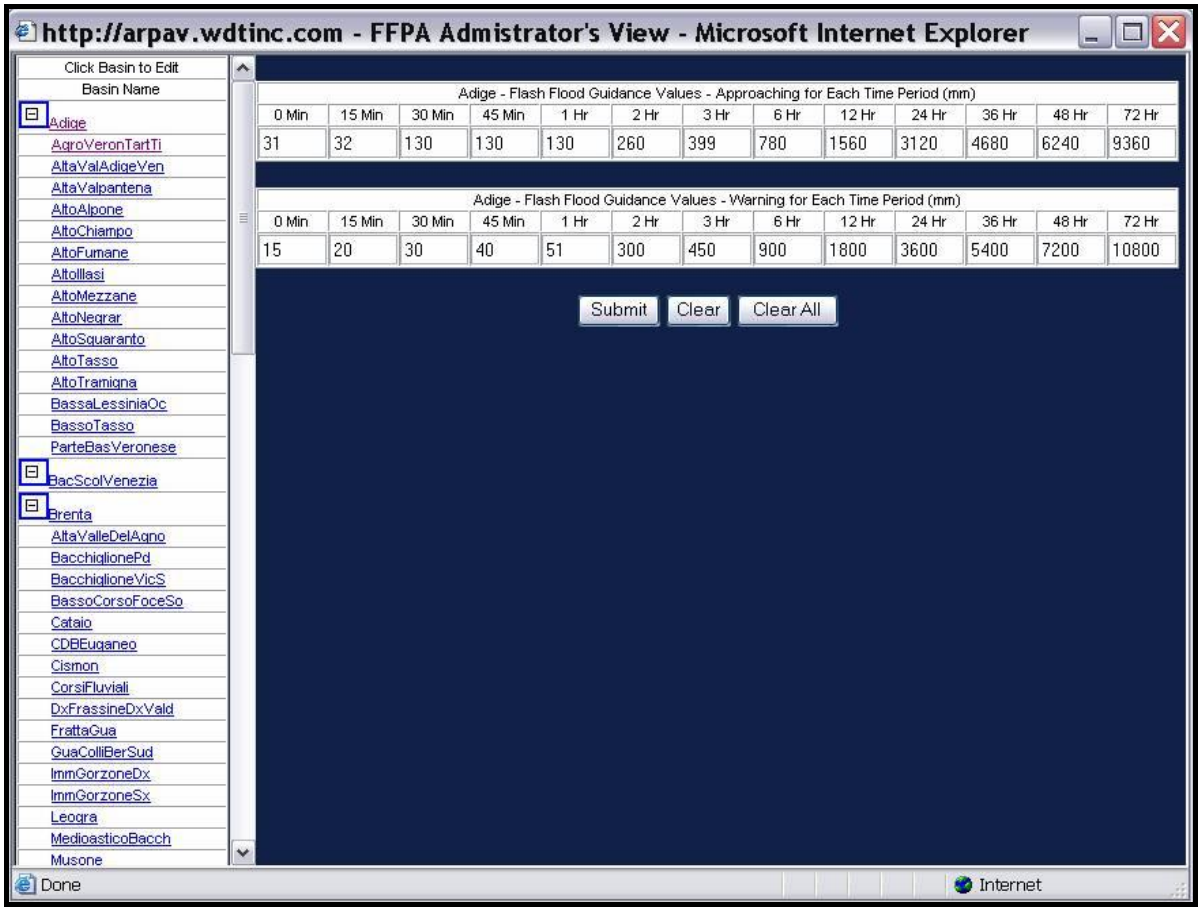

Figure 17. User interface to change Flash Flood Guidance values. These values are used in the FFPA algorithm for automated flash flood warnings.

2.6 Lightning Prediction Algorithm (LPA)

Figure 18 shows an example of the display from an LDSS installation in Greece for the Hellenic National Meteorological Service (HNMS). In this example lightning data is overlaid on a radar mosaic. The polygons in the image show areas where moderate lightning activity is forecast to occur in the next 60 minutes. These polygons are derived from the Lightning Prediction Algorithm (LPA). LPA is based on history of gridded lightning data and predicted in time using results from MAPLE.

Lightning data are interpolated to a high-resolution grid and flagged on number of detections per grid point. Extrapolation of the lightning data forward in time is then performed using MAPLE. Future enhancements to the system can include the combined use of radar and lightning data in MAPLE to produce more sophisticated lightning predictions. Moderate or high lightning activity is predicted based on the number of detections per grid point. Additionally, when atmospheric temperature data are coupled with lightning and radar data, areas of potential lightning (where lightning has yet to be detected) can be forecast using LPA.

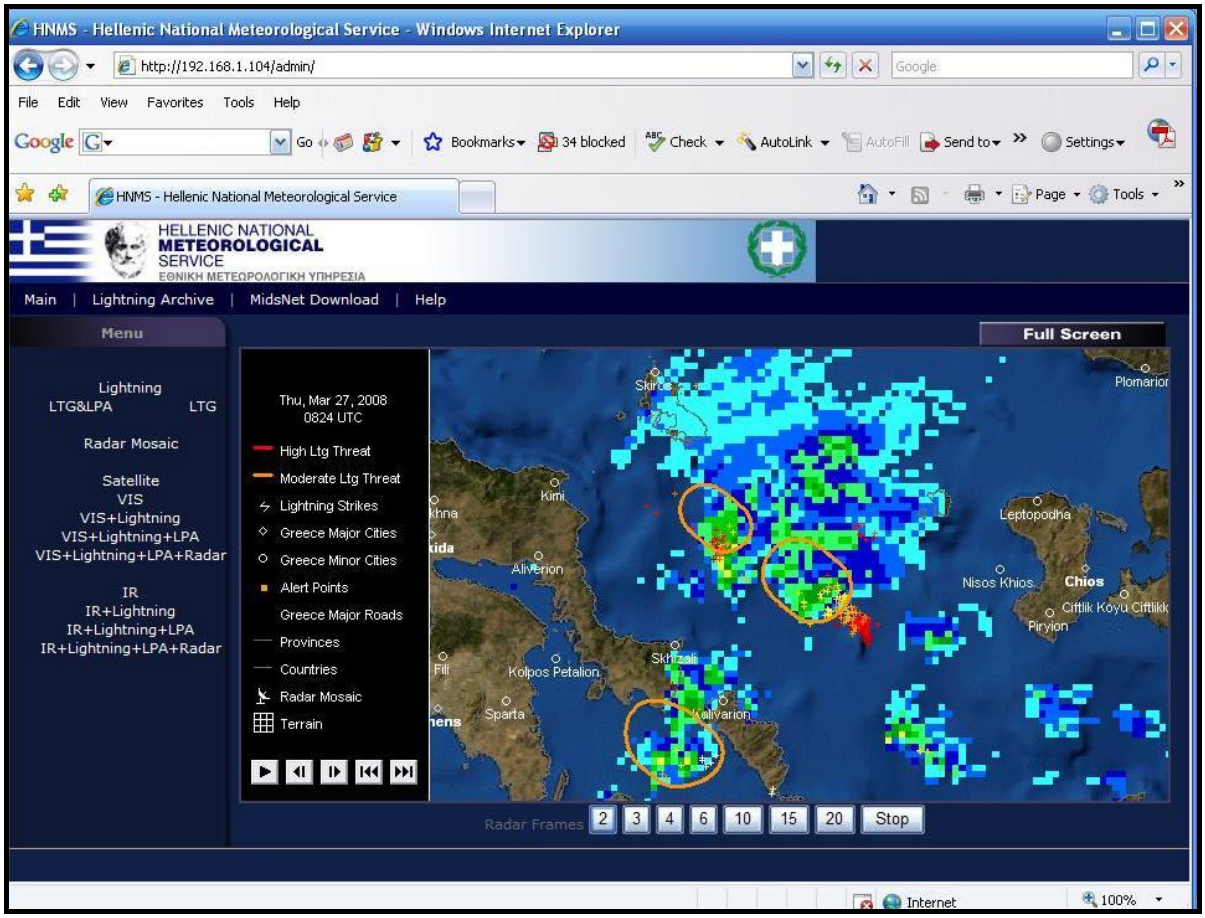

Figure 18. Example of LPA output from the WDT system in Greece. Yellow polygons depict 1 hour forecasts of threat areas expected to contain moderate lightning activity.

2.7 GIS Asset Monitoring System (GAMS)

The GIS-Based Asset Monitoring System (GAMS) utilizes a database of user assets to provide automated alerts of estimated time of arrival and departure (ETA/ETD) of hazardous weather to decision makers through the HDSS or NDSS displays and via email, cell phone, or PDAs. These asset locations in the database can either be point locations, line segments, or polygons. GAMS compares predicted threat areas with the location of each of the assets. If there is overlap between the predicted threat areas and an asset, an alarm is sent. The content of the alarm includes which asset is alerted and the ETA/ETD of the threat. The user can control what parameters to be alerted upon. Figure 19 shows an example of the GAMS output from a custom site built for an electric utility customer. In the figure a transformer station is being warned for lightning through a pop-up window.

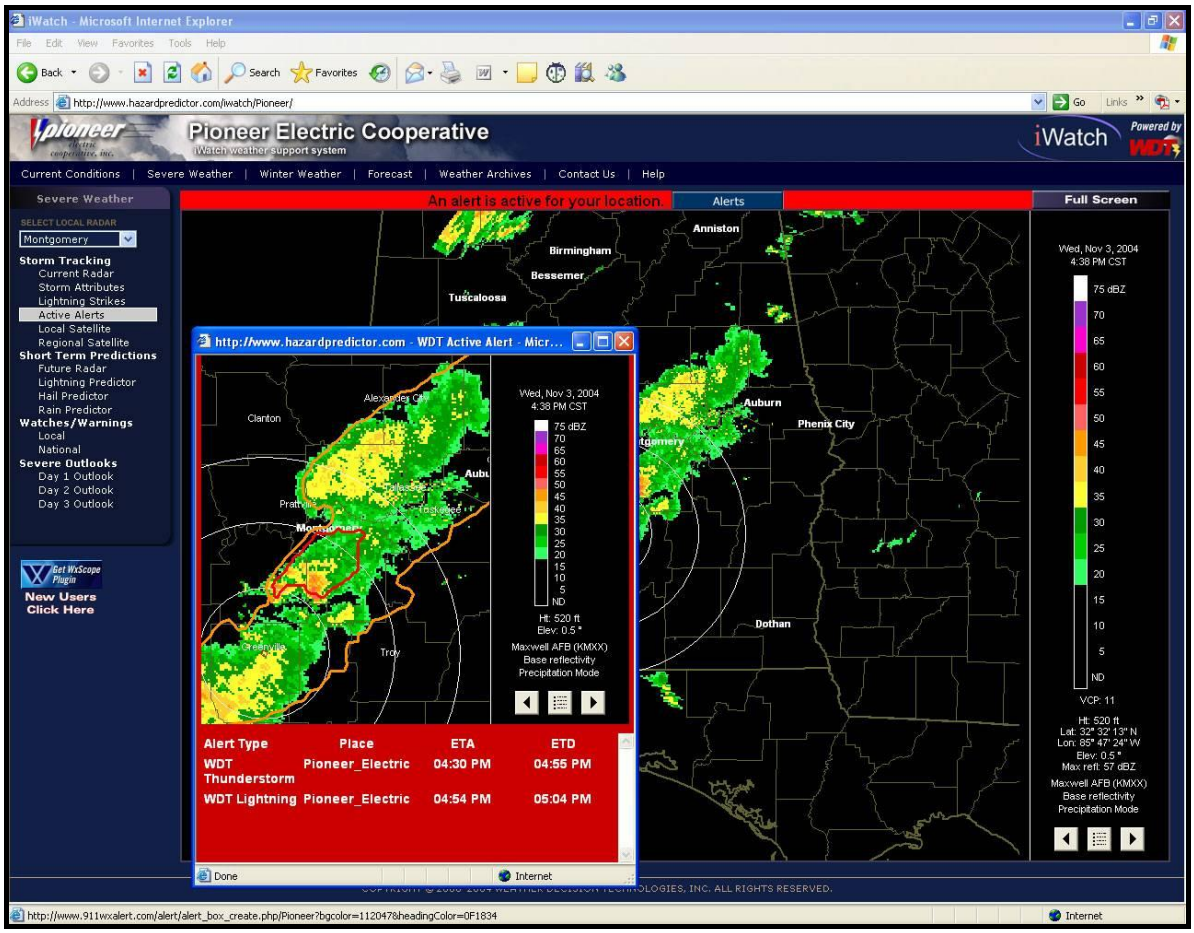

Figure 19. Example of GAMS alerting capability within a custom page. Insert shows pop-up window used for lighting alert with ETA/ETD information for one of the customer's assets.

2.8 Storm Cell Identification and Tracking (SCIT) Algorithm

The Storm Cell Identification and Tracking (SCIT) Algorithm was initially developed at NSSL and provided to the NEXRAD program. SCIT is a centroid tracking algorithm that tracks smaller scale features. SCIT searches volumetric radial data for reflectivity continuity among reflectivity gates for given dBZ values. Gates that fall within certain thresholds are grouped in the radial direction. Groupings are then performed in the azimuthal direction to produce 2-dimensional segments of common reflectivity values. Once all reflectivity segments are grouped in 2D in the horizontal plane, a vertical continuity search is performed. Given certain reflectivity and distance bounds, the 2D features are correlated in the vertical to give 3D storm centroid locations. Tracking is performed by applying a weighted least squares fit once a storm is identified for two consecutive volume scans. Figure 20 shows an example of SCIT output and table cell ranking.

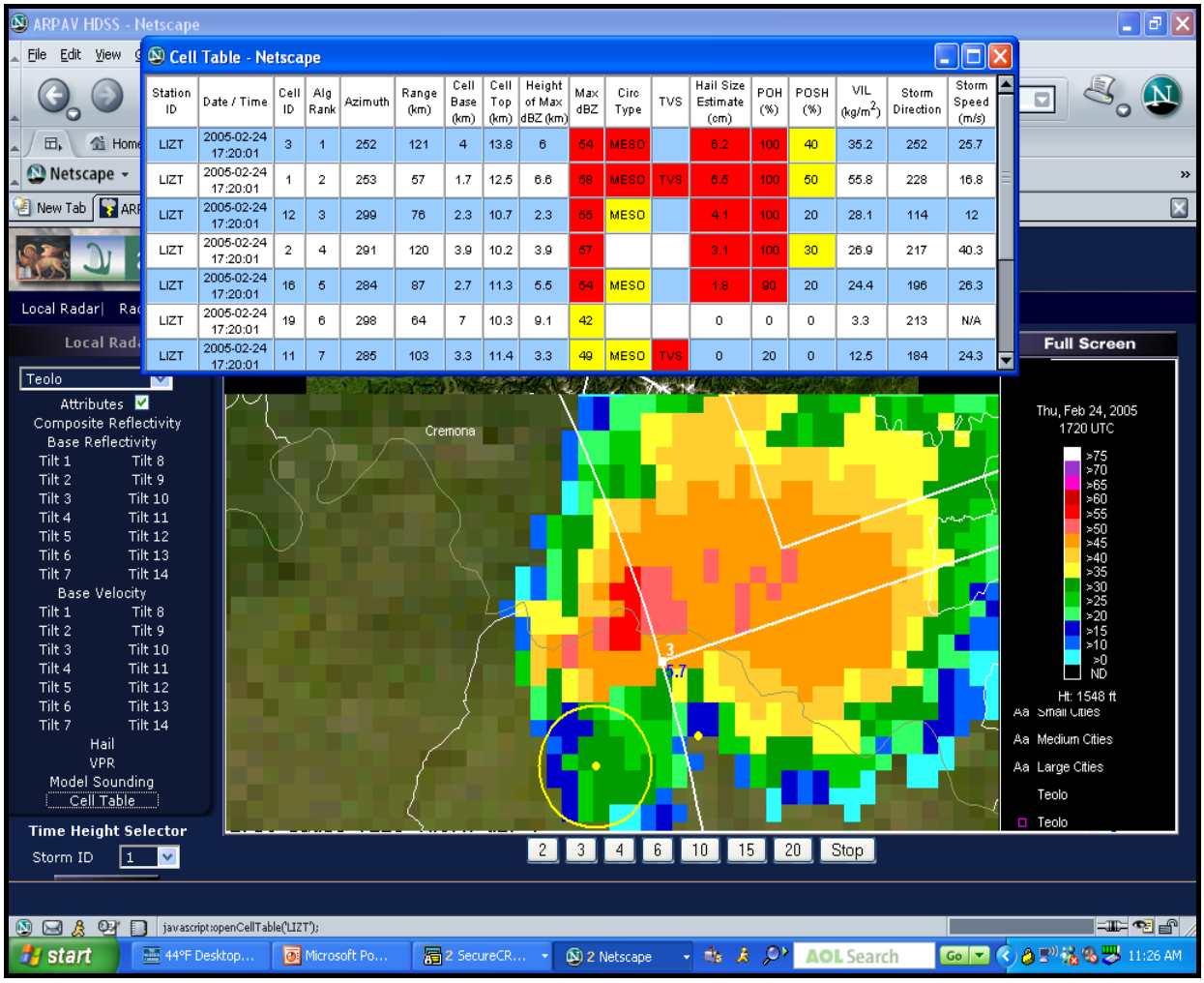

Figure 20. Example of SCIT output for cell forecasts and attributes. The white lines represent tracks. The insert shows output for each storm. The storms are ranked in order of severity.

2.9 Hailswath Predictor

The Hailswath Predictor™ is a WDT proprietary algorithm that utilizes output from the Storm Cell Tracker and the Hail Detection Algorithm (HDA) to predict the areal extent of hail in the next 30 minutes. An example of the output of the Hailswath Prediction Algorithm is shown in Figure 21.

The Hail Detection Algorithm provides an advanced approach to determining which storm cells are producing hail at the present time. The Hailswath Predictor builds upon this capability to provide highly accurate short-term predictions of hail. HDA was developed, tested, and verified extensively over several years. Studies show the tendency for hail producing storms to have certain reflectivity levels at observed heights above the freezing level. The Probability of Severe Hail (POSH), defined here as hail > ¾ inch in diameter, is found by calculating a parameter known as hail kinetic energy and using that parameter in a

weighting function that takes into account the heights of the 0 and –20 degree Celsius temperature levels. These levels are automatically updated using the most recent sounding and/or model data.

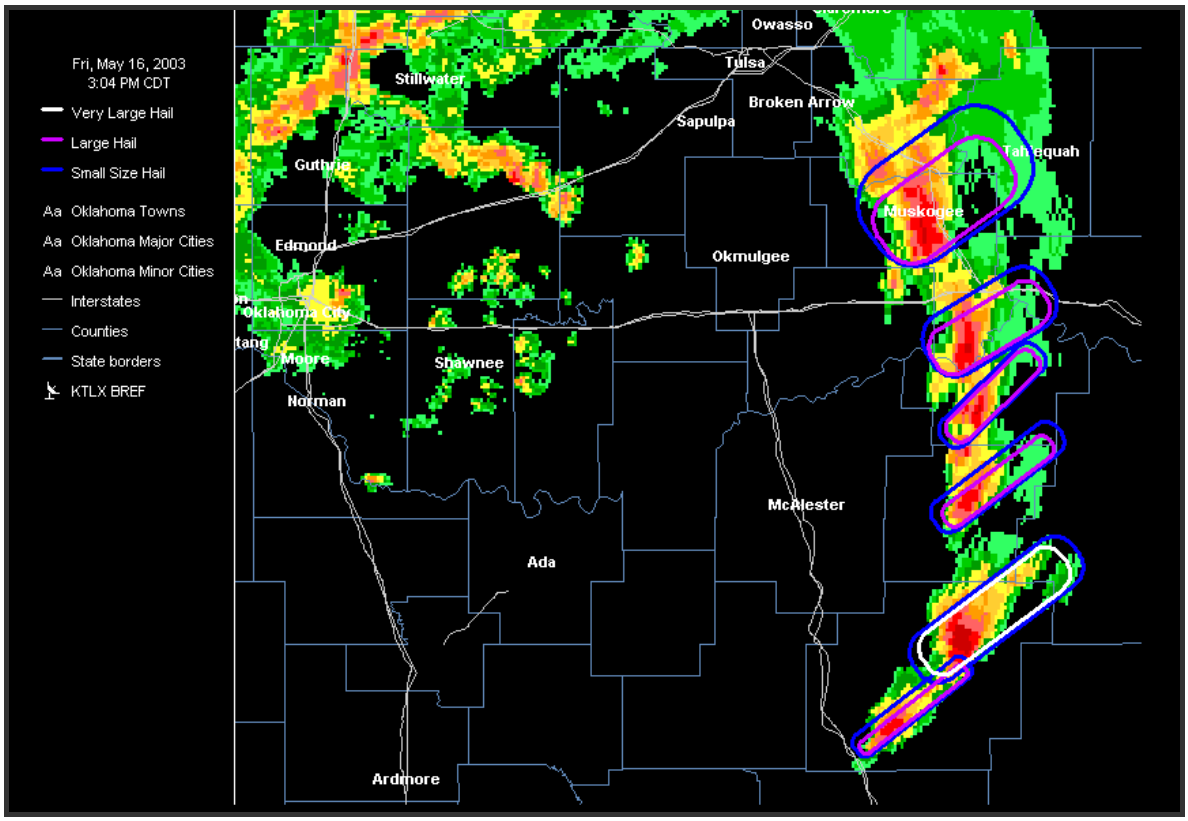

Figure 21. Output of Hailswath Predictor Algorithm. The blue polygons represent the areal prediction of hail of any size. Magenta is hailsize > 1 cm, white is hailsize > 2 cm.

3) Summary

This document has described the components and attributes of the HydroMet Decision Support System including implementation of HDSS internationally. HDSS encompasses meteorological data integration, Nowcasting and hydrometeorological algorithms, and display systems. HDSS contains several components such as data quality control, radar mosaics, gauge corrected QPE, flash flood prediction, automated alerting of hazardous conditions, and customized displays. Data and products from HDSS can be served to customized web page applications and mobile devices.

4) References

Germann, U. and I. Zawadzki, 2002: Scale-dependence of the predictability of precipitation from continental radar images. Part I: Description of methodology, *Mon. Wea. Rev.,* **130**, 2859-2873.

Gourley, J.J., R.A. Maddox, and B.M. Clarke, 2004: A multisensor approach to partitioning convective from stratiform echoes. *Preprints, 3rd European Conf. Radar Met.*, Visby, Sweden, 305-309.

Gourley, J.J., and C. Calvert, 2003: Automated detection of the bright band using WSR-88D data. *Wea. Forecasting*, **18**, 585-599.

Gourley, J.J., J. Zhang, R. A. Maddox, C.M. Calvert, and K. Howard 2001: A real-time precipitation monitoring algorithm - Quantitative Precipitation Estimation and Segregation Using Multiple Sensors (QPE-SUMS). *Preprints, Symp. On Precipitation Extremes: Predictions, Impacts, and Responses.* AMS, Albuquerque, NM, 57-60.

Lakshmanan V., T. Smith, G. J. Stumpf, and K. Hondl, The warning decision support system - integrated information, *Weather and Forecasting*, vol. 22, no. 3, pp. 596-612, 2007.

Lakshmanan V., T. Smith, K. Hondl, G. J. Stumpf, and A. Witt, A real-time, three dimensional, rapidly updating, heterogeneous radar merger technique for reflectivity, velocity and derived products, *Weather and Forecasting*, vol. 21, no. 5, pp. 802-823, 2006.

Lakshmanan V., A. Fritz, T. Smith, K. Hondl, and G. J. Stumpf, An automated technique to quality control radar reflectivity data, *J. Applied Meteorology*, vol. 4

Lakshmanan V., K. Hondl, and R. Rabin, An efficient, general-purpose technique for identifying storm cells in geospatial images, *J. Ocean. Atmos. Tech.*, vol. 26

Turner, B.J., I. Zawadzki, U. Germann, 2003: Scale-dependence of the Predictability of Precipitation from Continental Radar Images. Part III: Operational Nowcasting Implementation (MAPLE), Submitted to *Mon. Wea. Rev*

Zhang, J., K. Howard, and J.J. Gourley, 2005: Constructing three-dimensional multiple-radar reflectivity mosaics: Examples of convective storms and stratiform rain echoes. *J. Atmos. and Oceanic Tech.*, **22**, 30-43.

Zhang, J., S. Wang, and B. Clarke, 2004: WSR-88D reflectivity quality control using horizontal and vertical reflectivity structure. *Preprints, 11th Conf. Aviation, Range, and Areospace Met*., Hyannais, MA. AMS.About radar and meteorology. *J. Hydrometeor*. **6**, 532-549.